VOL. 10, NO. 6, APRIL 2015 ISSN 1819-6608
ARPN Journal of Engineering and Applied Sciences
©2006-2015 Asian Research Publishing Network (ARPN). All rights reserved.
www.arpnjournals.com

CALCULATION OF THE PARTICLE VELOCITY IN COLD SPRAY IN THE ONE-DIMENSIONAL NON-ISENTROPIC APPROACH

A. N. Ryabinin
Saint-Petersburg State University, Faculty of Mathematics and Mechanics, 28 University Ave., Petersburg, Russia
E-Mail: a.ryabinin@spbu.ru

ABSTRACT

The mathematical model of the motion of gas particles in De Laval nozzle in the one-dimensional non-isentropic approximation is considered. The model takes into account the exchange of momentum and energy between the gas and solid phases. We obtained a system of ordinary differential equations for the parameters of the gas and particle velocity and temperature. For the particular case of air as a carrier gas and copper particles, the system of equations is solved by the Runge-Kutta method. Inlet pressure was equal to $2.5\cdot 10^6$ Pa, inlet temperature was equal to 773 K. For particles of different diameters, the particle velocity and the temperature were calculated at the nozzle exit both in the isentropic and non-isentropic approximations. The ratio of particle and gas mass rates varied up to 20%. For small particle of 8 microns in diameter, exit particle velocity decreases from 691 m/s to 641 m/s, exit particle temperature increases from 113 K to 143 K, while ratio of mass rates arises from 0 to 20 %. For large particles, velocity difference is less than for small ones.

Keywords: cold gas dynamic spray, mathematical model, two-phase flow, de laval nozzle.

INTRODUCTION

Cold gas dynamic spraying (CGDS or cold spray) is a process in which powder particles of spraying material are injected within supersonic gas flow. Particles move at high speed in the gas stream and impact with the substrate material to form a coating [1, 2, 3]. Properties of the deposited coating and the deposition efficiency are determined by the speed and temperature of the particles at the time of impact [4, 5, 6, 7] and by substrate temperature [8, 9]. Carrier gases are accelerated up to supersonic velocities through converging-diverging De Laval nozzles.

Particles are injected in the carrier gas across either the nozzle inlet region or diverging part of the nozzle downstream the throat. In the first case, higher final velocities can be reached as they are entrained in the jet stream for a long period of time. On the other hand, when the particles are injected downstream the nozzle throat at low pressure zone, it is a more practical solution, but the impact speed reduces.

Most researchers separates the calculations of particle speed and temperature into two stages. In the first step, parameters of the gas are calculated in the nozzle and in the space between the nozzle and the substrate surface. In the second stage, the calculation of particle velocity and temperature is performed. It is usually assumed that the particle concentration is so low that particles have no influence on the characteristics of the gas flow [10 - 26]. Calculation of gas flows is carried out either based on one-dimensional isentropic approximation [11, 12, 19], or by Computational Fluid Dynamics (CFD) methods [10, 13 - 28]. Most of the CFD calculations were performed using the Fluent commercial software. The Lagrangian Discrete Phase Modeling (DPM) algorithm is implemented in Fluent. Thus, the calculation of the gas motion and the calculation of particle trajectory and particle velocity can be carried out sequentially by Fluent [13 - 15, 17 - 24, 27]. Samareh *et al*. [29] have studied the behavior of particles in De Laval nozzles and effects on gas velocity for high particle loadings (60 to 180 g/min), and by implementing advanced multiple equations Reynolds Stress Model. Such models can be accurate, but are relatively difficult to consistently converge up to higher order schemes [21].

Basics of one-dimensional isentropic method of gas velocity calculation in Laval nozzle are presented in papers [3, 4, 5]. The application of this method of calculation gives some overestimated values for the particle velocities, because there is thick boundary layer near the nozzle wall, so the one-dimensional approximation is not valid. However, the correction, proposed in papers [19, 30, 31] leads to the fact that the estimation of the particle velocity becomes accurate.

The flow in De Laval nozzle in the case of high concentration of particles is not adiabatic and isentropic because there is heat and momentum transfer between the gas and particles. In this paper, we proposed one-dimensional non-isentropic method of calculation of gas parameters in De Laval nozzle.

MATHEMATICAL MODEL

The equations of energy, momentum, mass and equation of state for ideal compressed gas are presented below:

$$\begin{aligned} &u\frac{d}{dx}\left(i+\frac{u^2}{2}\right)=Fu+q,\\ &u\frac{du}{dx}=F-\frac{1}{\rho}\frac{dp}{dx},\\ &\rho uA=\text{const},\\ &p=\rho RT, \end{aligned} \qquad (1)$$

where x is coordinate along axis of the nozzle; i is gas enthalpy; u is gas velocity; F is the specific force, acting on the gas from the accelerating particles; q is the heat received from particles by unit of gas mass; p, ρ and T are

ARPN Journal of Engineering and Applied Sciences
©2006-2015 Asian Research Publishing Network (ARPN). All rights reserved.
www.arpnjournals.com

pressure, density and temperature of the gas; A is area of the nozzle cross section; R is gas constant. Let take into account, that $i = \frac{\gamma}{\gamma - 1} RT$, $a^2 = \gamma R$. Here γ is the ratio of gas specific heats, a is a speed of sound. After transformation, equations (1) could be presented in the next form:

$$\frac{du}{dx} = \frac{q(\gamma-1) - Fu - ua^2\theta}{a^2 - u^2},$$
$$\frac{da}{dx} = \frac{\gamma-1}{2}\frac{Fa - q\left(\gamma u/a - a/u\right) + u^2 a\theta}{a^2 - u^2}, \quad (2)$$
$$\theta = \frac{1}{A}\frac{dA}{dx}.$$

The system of equations (2) should consider together with the equations of motion of the particles under the acting of aerodynamic force. Equations of motion of a single particle (3) is taken from the [6, 7].

$$\frac{d\nu_p}{dt} = \frac{3}{4}C_D\frac{\rho}{\rho_p}\frac{(u-\nu_p)|u-\nu_p|}{d},$$
$$\frac{dx}{dt} = \nu_p, \quad (3)$$
$$\frac{dT_p}{dt} = \frac{6\,\mathrm{Nu}\,k}{d^2\rho_p c}(T - T_p),$$

where v_p, ρ_p, T_p, d, c are velocity, density, temperature, diameter and specific heat of particle, Nu is Nusselt number, which depends on Reynolds number Re_p, Prandtl number Pr and Mach number M_p [27], C_D is drag coefficient, k is thermal conductivity,

$$\mathrm{Re}_p = \frac{\rho|u - v_p|d}{\mu}, \quad M_p = \frac{|u - v_p|}{a}.$$

Variable t in equations (3) can be replaced by variable x:

$$\frac{d\nu_p}{dx} = \frac{3}{4}C_D\frac{\rho}{\rho_p}\frac{(u-\nu_p)|u-\nu_p|}{d\nu_p},$$
$$\frac{dT_p}{dx} = \frac{6\,\mathrm{Nu}\,k}{d^2\rho_p c v_p}\left(\frac{a^2}{\gamma R} - T_p\right). \quad (4)$$

Thus, two systems of equations (3) and (4) are combined into one system (5):

$$\frac{du}{dx} = \frac{\delta fu^2 - \delta ucg(\gamma-1) - ua^2\theta}{a^2 - u^2},$$
$$\frac{da}{dx} = \frac{\gamma-1}{2}\frac{\delta guc(\gamma u/a - a/u) - \delta fau + u^2 a\theta}{a^2 - u^2},$$
$$\frac{dv_p}{dx} = f,$$
$$\frac{dT_p}{dx} = g, \quad (5)$$
$$\theta = \frac{1}{A}\frac{dA}{dx}, \quad f = \frac{3}{4}C_D\frac{\rho}{\rho_p}\frac{(u-v_p)|u-v_p|}{dv_p},$$
$$g = \frac{6\,\mathrm{Nu}\,k}{d^2\rho_p c v_p}\left(\frac{a^2}{\gamma R} - T_p\right).$$

Combining the two systems we use the relationships between F, q and f, g:

$$F = -\delta uf, \quad q = -\delta ucg.$$

Here δ is the ratio of particle and gas mass rates. Expression for Nusselt number was taken from [27]:

$$\mathrm{Nu} = 2 + 0.44\,\mathrm{Re}_p^{1/2}\,\mathrm{Pr}^{1/3}\exp(0.1 + 0.872\mathrm{M}_p).$$

This expression is only valid for $\mathrm{M}_p > 0.24$ and $T > T_p$. In all other cases, the Nusselt number does not depend on Mach number:

$$\mathrm{Nu} = 2 + 0.44\,\mathrm{Re}_p^{1/2}\,\mathrm{Pr}^{1/3}.$$

Expressions for drag coefficient C_D were taken from Henderson paper [32].

For isentropic flow ($\delta = 0$) at the nozzle throat ($\theta = 0$) gas velocity u is equal to the speed of sound a. For non-isentropic flow point of sonic conditions ($u = a$) is shifted from the throat. If $\delta << 1$, in the vicinity of sonic condition

$$\frac{du}{dx} = a_0\sqrt{\frac{1}{\gamma+1}\frac{d\theta}{dx}},$$
$$\frac{da}{dx} = -a_0\frac{\gamma-1}{2}\sqrt{\frac{1}{\gamma+1}\frac{d\theta}{dx}}, \quad (6)$$

and shift Δx is given by

$$\Delta x = \frac{\delta u[fu - cg(\gamma+1)]}{a^2 d\theta/dx}. \quad (7)$$

The system of ordinary differential equations (5) can be solved numerically.

ARPN Journal of Engineering and Applied Sciences
©2006-2015 Asian Research Publishing Network (ARPN). All rights reserved.
www.arpnjournals.com

CALCULATIONS

If particles are injected downstream the throat, the initial conditions should be set at point of particle injection. The initial particle velocity must be greater than zero. The flow upstream the point of injection can be determined in isentropic approach. The case of particle injection across the nozzle inlet region is more complex. In this case, initial conditions should be set at sonic point near the nozzle throat. Approximately gas parameters and particle velocity and particle temperature can be determined in isentropic approach.

We considered the second case. The nozzle had a circular cross-section, the length of the converging part was equal to 50 mm and length of diverging part was equal to 120 mm. The nozzle had the throat of 2.67 mm in diameter. Exit diameter of diverging part was equal to 5.3 mm. We calculated the flight of copper particles, injected across the inlet part of the nozzle. The diameter of particles was in the range from 8 μm to 125 μm. The inlet pressure $p_o = 2.5 \cdot 10^6$ Pa, inlet temperature $T_o = 773$ K. The ratio of particle and gas mass rates $0 < \delta < 0.2$. The carrier gas was air.

System of equations (5) was solved by fourth-order Runge-Kutta method. Code was written in Pascal. Initial conditions were set at sonic point upstream the throat of the nozzle. In the small vicinity of the sonic point first two equation of system (5) were replaced by equations (6). We performed calculation downstream and upstream the point of sonic condition. Figure-1 shows the dependence of gas velocity on the distance x from place of particle injection for particle loading 20%.

The dependence of particle velocity on distance x is presented in Figure-2. Difference between results of isentropic and non-isentropic calculations for small particles is greater, than for large particles.

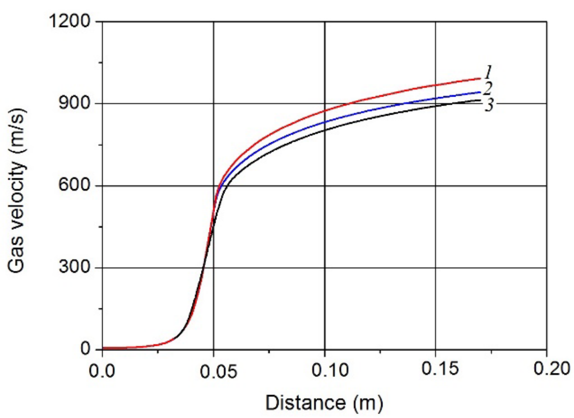

Figure-1. Gas velocity as a function of a distance from particle feeding ($\delta = 0.2$). *1* - isentropic approach, *2* - non-isentropic approach, particle diameter $d = 125$ μm, *3* - non-isentropic approach, particle diameter $d = 8$ μm.

At the nozzle exit for particles $d = 8$ μm velocity difference is equal to 50 m/s, while for particle $d = 125$ μm this difference reduces down to 15 m/s.

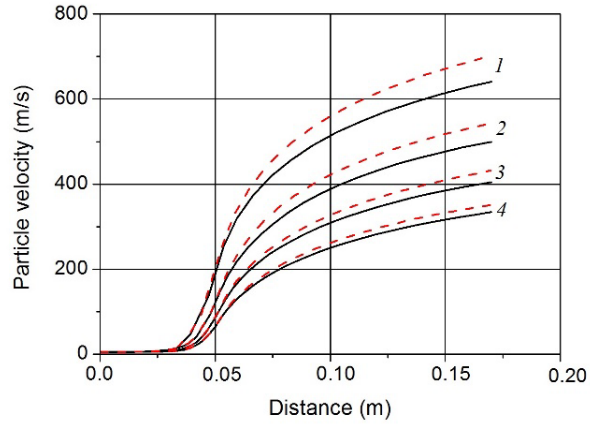

Figure-2. Particle velocity as a function of a distance from particle feeding ($\delta = 0.2$). Dash line - isentropic approach, solid line - non-isentropic approach. *1* - $d = 8$ μm, *2* - $d = 27$ μm, *3* - $d = 64$ μm, *4* - $d = 125$ μm.

Figure-3 demonstrates dependence of exit particle velocity on the ratio of particle and gas mass rates. One can see that this dependence is close to a linear one.

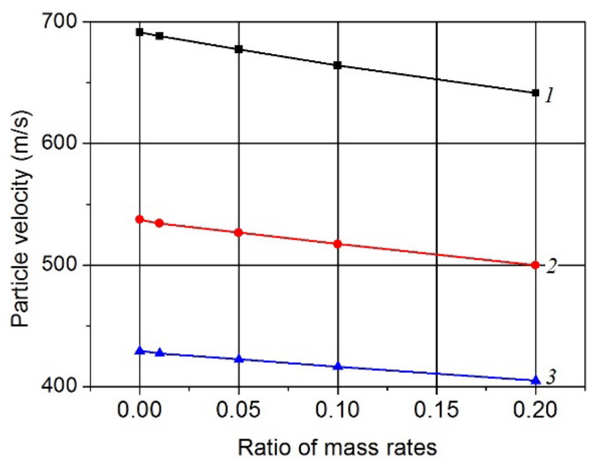

Figure-3. Exit particle velocity as a function of a ratio of mass rates δ. *1* - $d = 8$ μm, *2* - $d = 27$ μm, *3* - $d = 64$ μm.

Similar dependences are found for exit particle temperature. Figure-4 illustrates the exit particle temperature as function of a ratio of mass rates.

ARPN Journal of Engineering and Applied Sciences
©2006-2015 Asian Research Publishing Network (ARPN). All rights reserved.

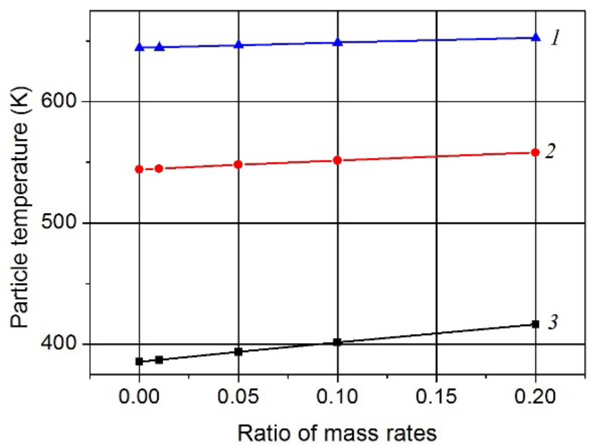

Figure-4. Exit particle temperature as a function of a ratio of mass rates δ. *1* - d = 64 μm, *2* - d = 27 μm, *3* - d = 8 μm.

At the nozzle exit for particles d = 8 μm particle temperature increases with arising of ratio of mass rates from 113 K to 143 K, for particle d = 64 μm the temperature increases from 372 K to 380 K only.

CONCLUSIONS

Basing on a one-dimension non-isentropic mathematical model of two-phase flow we analyzed the gas and particle velocities and particle temperatures. The momentum and energy transfer from the particles to gas leads the reducing of gas and particle velocities and arising of particle temperature.

REFERENCES

[1] Papyrin A., Kosarev V., Klinkov S., Alkhimov A., Fomin V. 2007. Cold spray technology, Elsevier Science, Amsterdam. p. 336.

[2] Irissou E., Legoux J.-G., Moreau C., Ryabinin A.N., Jodoin B. 2008. Review on cold spray process and technology: Part I. Intellectual property. Journal of Thermal Spray Technology. 17(4): 495-516.

[3] Dykhuizen R.C., Smith M.F. 1998. Gas dynamic principles of cold spray. Journal of Thermal Spray Technology. 7(2): 205-212.

[4] Assadi H., Schmidt T., Richter H., Kliemann J.-O., Binder K, Gärtner F., Klassen T., Kreye H. 2011. On parameter selection in cold spraying. Journal of Thermal Spray Technology. 20(6): 1161-1176.

[5] Schmidt T., Assadi H., Gartner F., Richter H., Stoltenhoff T., Kreye H., Klassen T. 2009. From particle acceleration to impact and bonding in cold spraying. Journal of Thermal Spray Technology. 18(5-6): 794-808.

[6] Wong W., Irissou E., Ryabinin A.N., Legoux J.-G., Yue S. 2011. Influence of helium and nitrogen gases on the properties of cold gas dynamic sprayed pure titanium coatings. Journal of Thermal Spray Technology. 20(1-2): 213-226.

[7] Wong W., VO P., Irissou E., Ryabinin A.N., Legoux J.-G., Yue S. 2013. Effect of particle morphology and size distribution on cold-sprayed pure titanium coatings. Journal of Thermal Spray Technology. 22(7): 1140-1153.

[8] McDonald M. G., Ryabinin A. N., Irissou E., Legoux J.-G. 2013. Gas-substrate heat exchange during cold-gas dynamic spraying. Journal of Thermal Spray Technology. 22(2-3): 391-397.

[9] Ryabinin A.N., Irissou E., McDonald A., Legoux J.-G. 2012. Simulation of gas-substrate heat exchange during cold-gas dynamic spraying. International Journal of Thermal Sciences. 56: 12-18.

[10] Jen T,-C., Li L., Cui W., Chen O., Zhang X. 2005. Numerical investigations on cold gas dynamic spray process with nano- and microsize particles. International Journal of Heat and Mass Transfer. 48: 4384-4396.

[11] Marrocco T., McCartney D.G., Shipway P.H., Sturgeon A.J. 2006. Production of titanium deposits by cold-gas dynamic spray: numerical modeling and experimental characterization. Journal of Thermal Spray Technology. 15(2): 263-272.

[12] Jodoin B., Raletz F., Vardelle M. 2006. Cold spray modeling and validation using an optical diagnostic method. Surface and Coatings Technology. 200: 4424-4432.

[13] Li W.-Y., Li C.-J., Wang H.-T., Li C.-X., Bang H.-S. 2006. Measurement and numerical simulation of particle velocity in cold spraying. Journal of Thermal Spray Technology. 15(4): 559-562.

[14] Karimi M., Fartaj A., Rankin G., Vanderzwet D., Birtch W., Villafuerte J. 2006. Numerical simulation of the cold gas dynamic spray process. Journal of Thermal Spray Technology. 15(4): 518-523.

[15] Li W.-H., Liao H., Douchy G., Coddet C. 2007. Optimal design of a cold spray nozzle by numerical analysis of particle velocity and experimental validation with 316L stainless steel powder. Materials and Design. 28: 2129-2137.

[16] Katanoda H., Fukuhara M., Iino N. 2007. Numerical study of combination parameters for particle impact velocity and temperature in cold spray. Journal of Thermal Spray Technology. 16(5-6): 627-633.

ARPN Journal of Engineering and Applied Sciences
©2006-2015 Asian Research Publishing Network (ARPN). All rights reserved.

[17] Samareh B., Dolatabadi A. A. 2007. Three-dimensional analysis of the cold spray process: the effects of substrate location and shape. Journal of Thermal Spray Technology. 16(5-6): 634-642.

[18] Schmidt T., Assadi H., Gartner F., Richter H., Stoltenhoff T., Kreye H., Klassen T. 2009. From particle acceleration to impact and bonding in cold spraying. Journal of Thermal Spray Technology. 18(5-6): 794-808.

[19] Klinkov S.V., Kosarev V.F., Sova A.A., Smurov I. 2009. Calculation of particle parameters for cold spraying of metal-ceramic mixtures. Journal of Thermal Spray Technology. 18(5-6): 944-956.

[20] Ning X.-J., Wang Q.-S., Ma Z., Kim H.-J. 2010. Numerical study of in-flight particle parameters in low-pressure cold spray process. Journal of Thermal Spray Technology. 19(6): 1211-1217.

[21] Lupoi R., O'Neill W. 2011. Powder stream characteristics in cold spray nozzles. Surface and Coatings Technology. 206: 1069-1076.

[22] Sova A., Okunkova A., Grigoriev S., Smurov I. 2013. Velocity of the particles accelerated by a cold spray micronozzle: experimental measurements and numerical simulation. Journal of Thermal Spray Technology. 22(1): 75-80.

[23] Yin S., Liu Q., Liao H., Wang X. 2014. Effect of injection pressure on particle acceleration, dispersion and deposition in cold spray. Computational Materials Science. 90: 7-15.

[24] Sova A., Grigoriev S., Kochetkova A., Smurov I. 2014, Influence of powder injection point position on efficiency of powder preheating in cold spray: numerical study. Surface and Coatings Technology. 242: 226-231.

[25] Champagne V.K., Helfritch D.J., Dinavahi S.P.G., Leyman P.F. 2011, Theoretical and experimental particle velocity in cold spray. Journal of Thermal Spray Technology. 20(3): 425-431.

[26] Suo X.K., Liu T.K., Li W.Y., Suo Q.L., Planche M.P., Liao H.L. 2013. Numerical study on the effect of nozzle dimension on particle distribution in cold spraying. Surface and Coatings Technology. 220: 107-111.

[27] Stoltenhoff T., Kreye H., Richter H.J. 2002. An analysis of the cold spray process and its coatings. Journal of Thermal Spray Technology. 11(4): 542-550.

[28] Fukumoto M., Terada H., Mashiko M., Sato K., Yamada M., Yamaguchi E. 2009. Deposition of copper fine particle by cold spray process. Materials Transactions. 50(6): 1482-1488.

[29] Samareh B., Stier O., Lüthen V., Dolatabadi A. 2009. Assessment of CFD modeling via flow visualization in cold spray process. Journal of Thermal Spray Technology. 18(5-6): 934-943.

[30] Alkhimov A.P., Kosarev V.F., Klinkov S.V. 2001. The features of cold spray nozzle design. Journal of Thermal Spray Technology. 10(2): 375-381.

[31] Kosarev V.F., Klinkov S.V., Alkhimov A.P., Papyrin A.N. 2003. On some aspects of gas dynamics of the cold spray process. Journal of Thermal Spray Technology. 12(2): 265-281.

[32] Henderson C.B. 1976. Drag coefficients of spheres in continuum and rarefied flows. AIAA Journal. 14(6): 707-708.